Non-tubular bonded joint under torsion: Theory and numerical validation

Nicola Pugno†

Department of Structural Engineering, Politecnico di Torino, Italy

Giuseppe Surace‡

Department of Aeronautical and Space Engineering, Politecnico di Torino, Corso Duca degli Abruzzi 24, 10129 Torino, Italy

Abstract. The paper analyzes the problem of torsion in an adhesive non-tubular bonded *single-lap* joint. The joint considered consists of two thin rectangular section beams bonded together along a side surface. Assuming the materials involved to be governed by linear elastic laws, equilibrium and compatibility equations were used to arrive at an integro-differential relation whose solution makes it possible to determine torsional moment section by section in the bonded joint between the two beams. This is then used to determine the predominant stress and strain field at the beam-adhesive interface (stress field along the direction perpendicular to the interface plane, equivalent to the applied torsional moment and the corresponding strain field) and the joint's elastic strain (absolute and relative rotations of the bonded beam cross sections). All the relations presented were obtained in closed form. Results obtained theoretically are compared with those given by a three dimensional finite element numerical model. Theoretical and numerical analysis agree satisfactorily.

Key words: non-tubular; single-lap; bonded joint; adhesive; torsion.

1. Introduction

The use of light alloys and composite materials is spreading in automotive and mechanical applications, as well as in aircraft construction. In addition, the development of epoxy resin-based adhesives has brought a wide range of advantages, such as adhesives make it possible to reduce structural weight, prevent the onset of corrosion, achieve better stress distribution in the adhesive layer, join dissimilar materials (e.g., steel and composites), and produce smooth surface contours, a major benefit for components exposed to a fluid current. All of these advantages encourage the designer to consider adhesive bonding for structures which until recently were joined using conventional techniques such as riveting, welding or threaded connections.

The drawbacks associated with adhesives in the past, including their limited service temperature range and susceptibility to chemical attack, have to a large extent been overcome.

As the literature indicates, studies have hitherto concentrated on the effects of perpendicular stress,

† Researcher
‡ Associate Professor

bending moments and shear on adhesive bonded joints. In certain situations, however, such joints are also subject to a torsional moment. Research in this area is restricted to tubular structures, as other cases are entirely lacking in the literature. A detailed bibliography of the literature on adhesive bonded joints under torsion is given in this paper. The lack of work on non-tubular joints indicated by this bibliography motivated the investigation presented in the work developed by Pugno (1998), which was used as the basis for the works of Pugno (1999) and Pugno, Surace (1998b, c), as well as for this paper.

This gap in the literature can perhaps be explained by noting that non-tubular adhesive bonded joints are not designed to withstand a torsional moment, which can thus induce a non-shearing stress state in the adhesive of such joints. As is well known, in fact, adhesive is by nature less effective when subjected to normal stresses (as is illustrated by the differences encountered when attempting to separate two pieces of adhesive tape by applying tensile or shear stresses). Though this is likely to be the major reason that little work has been done with non-tubular joints, it cannot be considered a justification. During its service life, in fact, a non-tubular adhesive bonded joint can find itself called upon to withstand accidental torsional loading: as the joint is not designed for this type of characteristic of internal reaction (the joint should be designed to tensile loading), even modest torsional loads can prove to be critical.

2. Theoretical model

2.1. Equilibrium equations

The bonded joint consisting of two elements and the interposed adhesive is considered to be subject to a torsional moment as shown in the Fig. 1:

Under these conditions, it is possible to isolate an element of infinitesimal length dx ($-c \le x \le +c$) belonging to the first beam and impose rotational equilibrium around the barycentric axis of the cross sections parallel to the x axis (Fig. 2):

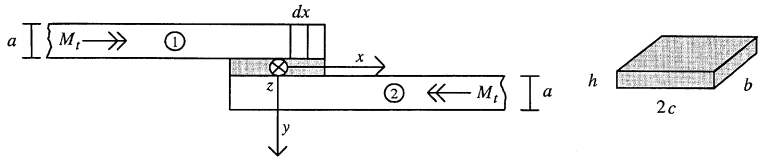

Fig. 1 Structural layout

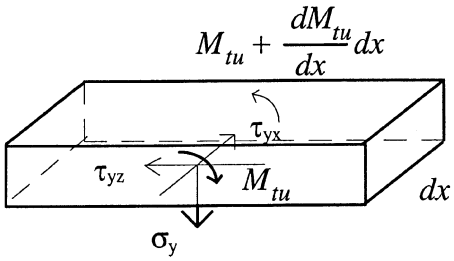

Fig. 2 Element of infinitesimal length

$$-\frac{dM_{tu}(x)}{dx}dx-\int_{-b/2}^{+b/2}\sigma_y(x,z)zdzdx+\int_{-b/2}^{+b/2}\tau_{yz}(x,z)\frac{a}{2}dzdx=0 \quad (1)$$

In order to satisfy translation equilibrium along the z axis the last integral must be zero.

The increase in torsional moment is balanced by normal stresses σ_y. The underlying adhesive element will thus be stressed in the area of contact with the two beams by a stress field equivalent to this increase.

2.2. Constitutive laws and kinematic hypothesis

It is assumed that all three of the materials making up the joint (beams and adhesive) are governed by a linear elastic law (isotropic). While this is intuitively obvious for the beams (which are typically metal), this is not the case for the adhesive, which is more likely to show a typically nonlinear behavior. Under torsion, however, the stress state in the adhesive created in a non-tubular bonded joint is basically normal. As it is well known that adhesive can withstand shear stresses which are an order of magnitude higher than the ultimate normal stresses, we can conclude that the stress values occurring during service for the condition considered herein are low. It is precisely because of these low stresses that we can assume also for the adhesive a linear elastic law. This linear behavior is experimentally well-shown (Pugno 1998).

In addition, the low stresses exchanged via the adhesive between the two beams also make it possible to assume that the latter also behave as de Saint Venant solids in the bond area (Technical theory of beams).

Under these assumptions, the adhesive's specific dilation ε_y will be linear along the joint thickness (z axis), given that, unless warping occurs, the adhesive will connect two rigidly rotated beam cross sections (Fig. 3). The strain assumption which was made concerning rigid cross section rotation is compatible with warping in the section: while beam kinematics will in fact cause the section to warp (longitudinal displacements), along the y and z co-ordinates the displacements can effectively be expressed as a rigid rotation around the center of torsion, which in this case coincides with the section's centroid. In any case the warping in the two beams, as first approximation, will be negligible, since the two beams have a thin rectangular cross section (but for a T section, for example, this could be not negligible).

As consequence this dilation ε_y is the predominant strain field in the adhesive (Fig. 3) and, as first

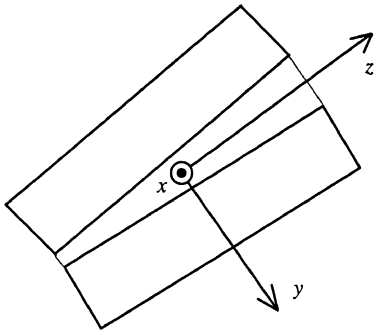

Fig. 3 Kinematic resulting from rigid rotation of the cross sections of the two beams

approximation, the normal strain fields ε_x and ε_z will be negligible by comparison. This, which in any case is intuitively obvious, is also clear from numerical analysis (Pugno 1998).

The corresponding predominant stress field σ_y will be equivalent to the applied torsional moment. Determining this stress field is thus of paramount interest.

In view of the assumptions made concerning strains and the linear elastic laws governing the materials, the predominant stress field will be linear along the joint thickness (z coordinate), as will be the corresponding specific dilation.

For the equilibrium Eq. (1) to be satisfied, bearing in mind that the stress field perpendicular to the beam-adhesive contact surface is linear along z, it must be possible to write the following equation:

$$\sigma_y(x, z)=-\frac{dM_{tu}(x)}{dx}\frac{z}{I_x^*} \tag{2}$$

where $I_x^*=\frac{b^3}{12}$ is a moment of inertia per unit length.

The strain field in the adhesive is obtained from the linear elastic law $\sigma_y(\varepsilon_y, \varepsilon_{x,z}\cong 0)$ governing the adhesive material, given by the following relation:

$$\varepsilon_y(x, z)=\frac{(1+\nu_a)(1-2\nu_a)}{(1-\nu_a)E_a}\sigma_y(x, z)=\frac{\sigma_y(x, z)}{E_a^*}=-\frac{dM_{tu}(x)}{dx}\frac{z}{E_a^* I_x^*} \tag{3}$$

being E_a, ν_a the Young's and Poisson's moduli for the adhesive (E_a^* is its fictitious Young's modulus).

2.3. Compatibility equation

The torsional moment $M_{tu}(x)$ in the joint between the two beams can be written as:

$$M_{tu1}(x)=M_t f(x) \tag{4}$$

$$M_{tu2}(x)=M_t(1-f(x)) \tag{5}$$

as the sum of the moments absorbed by the two elements must be equivalent to the applied torsional moment M_t.

Function $f(x)$ has the real range $[-c, +c]$ as its domain and, in order for the boundary conditions for the torsional moments

$$M_{tu1}(-c)=M_t \qquad M_{tu1}(+c)=0 \tag{6}$$

$$M_{tu2}(-c)=0 \qquad M_{tu2}(+c)=M_t \tag{7}$$

to be satisfied, must be unity at the extreme left and zero at the extreme right of the domain.

Function $f(x)$, and thus the torsional moment absorbed by the two elements at the joint, can be found thanks to the compatibility established for the rotations of the two beam cross sections. These rotations are expressed as follows:

$$\theta_1(x)=\int_{-c}^{x}\frac{M_{tu1}(t)}{GI_t}dt+\theta_1^0 \tag{8}$$

Table 1 Coefficient β as a function of the ratio b/a

b/a	1	1.5	2	3	10	∞
$\beta(b/a)$	0.141	0.196	0.229	0.263	0.312	1/3

$$\theta_2(x)=\int_{-c}^{x}\frac{M_{tu2}(t)}{GI_t}dt+\theta_2^0 \tag{9}$$

as G is the shear elastic modulus, I_t is the factor of torsional rigidity for each beam, and θ_i^0 is the absolute rotation of the initial section ($x=-c$) of beam i. Through an appropriate choice of reference system, we can always have $\theta_1^0=0$ (rotations calculated starting from the strained configuration of the first element's initial section).

The factor of torsional rigidity for a rectangular section can be expressed through a tabular coefficient (Table 1) as a function of the ratio of the lengths of the major and minor sides of the section as indicated below (in the considered case, $\beta\sim1/3$):

$$I_t=\beta\left(\frac{b}{a}\right)a^3b \tag{10}$$

Assuming linearity for the adhesive, the compatibility equation dictates that the infinitesimal moment $dM_{tu}(x)$ occurring at the ends of an adhesive element and equivalent to the stresses exchanged at the interface zones be proportionate to the variation in rotation between the element's bases (interface segments, Fig. 4).

The compatibility equation is written as:

$$\frac{dM_{tu1}(x)}{dx}=K^*(\theta_1(x)-\theta_2(x))=-K^*\Delta\theta(x) \tag{11}$$

with K^* as the adhesive's stiffness per unit length. This can be determined with reference to Fig. 4, from which it is possible to conclude that the following relation is valid ($\tan(\Delta\theta/2)\cong\Delta\theta/2$):

$$\varepsilon_y\left(x,z=\frac{b}{2}\right)\frac{h}{2}=\frac{b}{2}\frac{\Delta\theta(x)}{2} \tag{12}$$

Inserting Eq. (3) in Eq. (12) and through comparison with Eq. (11), the expression for the adhesive's stiffness is obtained:

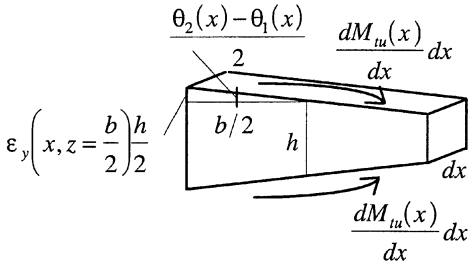

Fig. 4 Adhesive element belonging to a cross section under strain

$$K^*=\frac{E_a^* I_x^*}{h} \tag{13}$$

3. Solution of the problem

Inserting the rotation expressions (8) and (9) in the compatibility Eq. (11) gives the integro-differential relation:

$$\frac{dM_{tu1}}{dx}(x)=K^*\int_{-c}^{x}\frac{M_{tu1}(t)-M_{tu2}(t)}{GI_t}dt-K^*\theta_2^0 \tag{14}$$

This relation can be expressed with a single unknown $f(x)$, remembering the relations (4, 5), derivation gives the following second order differential equation in $f(x)$:

$$\frac{d^2f(x)}{dx^2}-\frac{2K^*}{GI_t}f(x)=-\frac{K^*}{GI_t}\qquad\begin{cases}f(-c)=1\\ f(c)=0\end{cases} \tag{15}$$

Table 2 Analytical relations

$A=\sqrt{\frac{2K^*}{GI_t}}$	$K^*=\frac{E_a^* I_x^*}{h}$	$E_a^*=\frac{(1-\nu_a)E_a}{(1+\nu_a)(1-2\nu_a)}$	$I_x^*=\frac{b^3}{12}$	$I_t=\beta\left(\frac{b}{a}\right)a^3 b$
Torsional moments $f(x)$			$M_{tu1}(x)=M_t f(x)$ $M_{tu2}(x)=M_t(1-f(x))$ $f(x)=\frac{1}{2}\left(1-\frac{\sinh(Ax)}{\sinh(Ac)}\right)$	
Stress and strain $\frac{df(x)}{dx}$			$\sigma_y(x,z)=-\frac{M_t}{I_x^*}z\frac{df(x)}{dx}$ $\varepsilon_y(x,z)=-\frac{M_t}{E_a^* I_x^*}z\frac{df(x)}{dx}$ $\frac{df(x)}{dx}=-\frac{A}{2}\frac{\cosh(Ax)}{\sinh(Ac)}$	
Rotations $\int_{-c}^{x}f(t)dt$			$\Delta\theta(x)=\theta_2(x)-\theta_1(x)=-\frac{M_t}{K^*}\frac{df(x)}{dx}$ $\theta_1(x)=\frac{M_t}{GI_t}\int_{-c}^{x}f(t)dt$ $\theta_2(x)=\frac{M_t}{GI_t}\int_{-c}^{x}(1-f(t))dt+\frac{M_t}{\sqrt{2GI_tK^*}}c\tanh(Ac)$ $\int_{-c}^{x}f(t)dt=\frac{1}{2}(x+c)+\frac{1}{2A}\left(c\tanh(Ac)-\frac{\cosh(Ax)}{\sinh(Ac)}\right)$	

This differential equation, together with the boundary conditions shown alongside, make it possible to determine the torsional moment section by section at the overlap. Using Eqs. (2) and (3) yields the predominant strain and stress field. Relations (8, 9, 11) yield joint strain in terms of absolute and relative rotations. Comparing the differences between Eq. (8) and Eq. (9) and Eq. (11) makes it possible to determine constant θ_2^0 once the reference system has been established with $\theta_1^0=0$.

The analytical relations which were obtained are presented in Table 2. For each relation, a qualitative curve is plotted. Fig. 5 shows the curve for the function $f(x)$ governing torsional moment transmission in the joint, while Fig. 6 shows its derivative, which governs relative rotations and stresses in a constant z plane. Fig. 7 illustrates its integral governing absolute rotations, and Fig. 8 illustrates stresses on the bond plane. Fig. 9 presents the most common nondimensionalized curves for $f(x)$, its derivative and its integral; the maximum value of the plotted function is shown for each of the preceding figures.

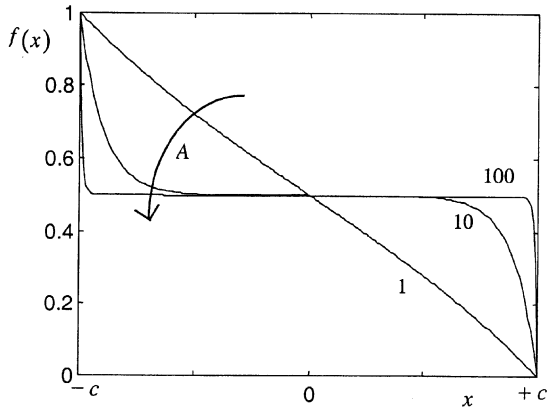

Fig. 5 Qualitative curve for $f(x)$ (torsional moments)

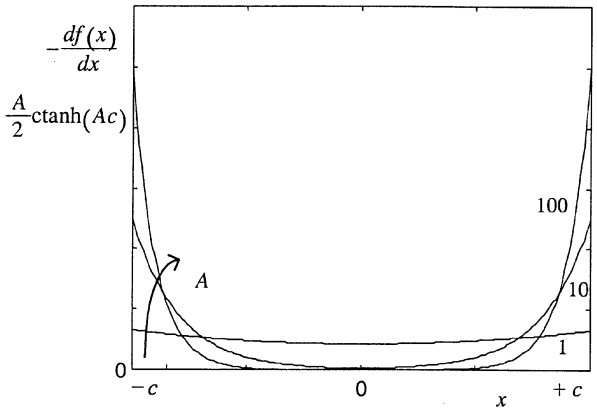

Fig. 6 Qualitative curve for $-\frac{df(x)}{dx}$ (relative rotations)

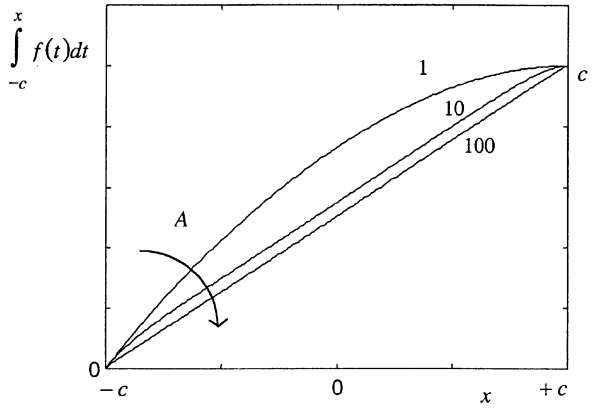

Fig. 7 Qualitative curve for $\int_{-c}^{x} f(t)dt$ (absolute rotations)

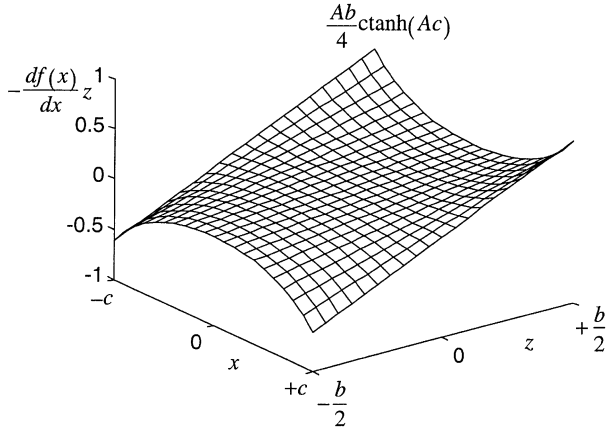

Fig. 8 Qualitative surface $-\frac{df(x)}{dx}z$ (stresses and strains)

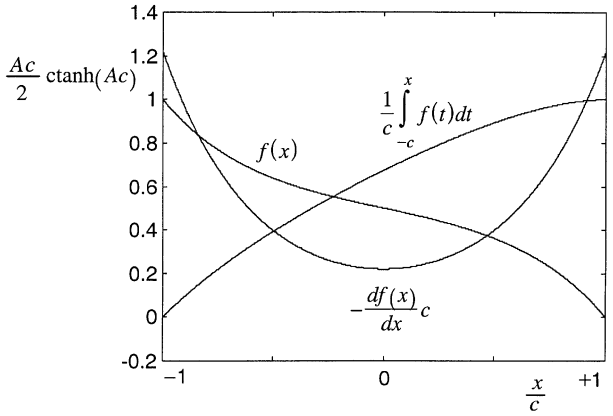

Fig. 9 Nondimensionalized qualitative curves for the function $f(x)$, the opposite of its derivative and its integral for common bonded joints (nondimensionalized constant Ac=2.4)

4. Stress concentration factor and gain parameter

In the light of the formulas found above, a stress concentration factor can be defined which indicates the extent to which maximum stress departs from the mean. Focusing attention on the plane $z=b/2$ (critical), the stresses are:

$$\sigma_y(x)=-\frac{M_t}{I_x^*}\frac{b}{2}\frac{df(x)}{dx} \tag{16}$$

and their mean value is:

$$\sigma_{y_{\text{mean}}}=\frac{1}{2c}\int_{-c}^{+c}\sigma_y(x)dx=\frac{M_t}{I_x^*}\frac{b}{4c} \tag{17}$$

With $A=\sqrt{\frac{2K^*}{GI_t}}$, the maximum stress is given by:

$$\sigma_{y_{\max}}=\sigma_y(x=c)=\frac{M_t Ab}{I_x^* 4}c\tanh(Ac) \tag{18}$$

Consequently, the stress concentration factor is given by:

$$\lambda=\frac{\sigma_{y_{\max}}}{\sigma_{y_{\text{mean}}}}=c\tanh(Ac)Ac \tag{19}$$

Greater interest attaches to the gain parameter λ^*, i.e., the index of the gain in maximum stress levelling which can be obtained by increasing the bond length. In this connection, it should be noted that as the bond length tends to infinity, the maximum stress tends asymptotically to a minimum nonzero value.

$$\sigma_{y_{\max}}|_{\min}=\lim_{c\to\infty}\sigma_{y_{\max}}=\frac{M_t}{I_x^*}\frac{Ab}{4} \tag{20}$$

The gain parameter can thus be defined as:

$$\lambda^*(Ac)=\frac{\sigma_{y_{\max}}|_{\min}}{\sigma_{y_{\max}}}=\tanh(Ac) \tag{21}$$

and must be as close to unity as is compatible with the need for a compact joint. Under this assumption the stress concentration factor, prudently overestimated, is detailed as follows:

$$\lambda\cong Ac \quad \text{for} \quad \lambda^*\cong 1 \tag{22}$$

Fig. 10 shows that gain parameter λ^* presents little variation after a certain value of the nondimensionalized parameter Ac (~3); consequently, further increases in bond length are pointless for the torsional load. Under these assumptions the stress concentration factor appears close to three, a well-known numerical value in elastic problems. However it should be borne in mind that the bond length depends prevalently on the tensile load for which the joint is designed.

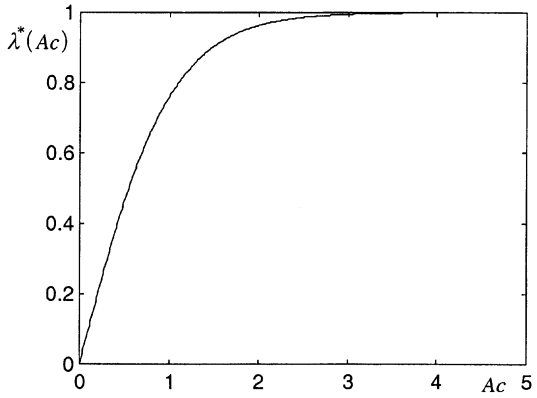

Fig. 10 Gain parameter $\lambda^*(Ac)$

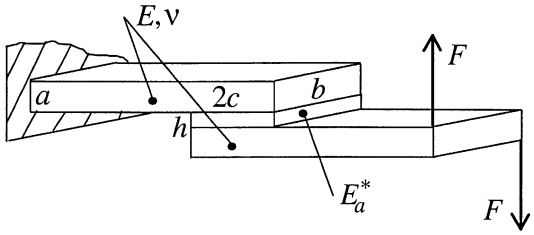

Fig. 11 *Single-lap* joint investigated using the FEM code

In order to obtain a unit value for the stress concentration factor given by Eq. (19) it is possible to modify the joint profile (Pugno 1999). This is achieved by chamfering the edges, which are in any case not involved in the stress flow induced by a tensile load. The corresponding joint is optimized for uniform torsional strength and is thus both lighter and stronger.

5. Numerical validation

The ANSYS 5.3 code was used for numerical finite element analysis in the work of Pugno (1998). The simulated three dimensional model is shown in Fig. 11.

The finite element used is the *brick* (a square prism element with 20 nodes, in the vertices and centers of the edges) which makes it possible to consider parabolic shape functions.

The adhesive is divided into $8 \times 8 \times 3=192$ elements. In this context the surface shown in Fig. 8 is numerically obtained using $17 \times 17=289$ nodes to have a sufficient number of points to estimate the stress field and the concentration factors (not-singular) at the four corners. Each of the two beams, along the overlap zone, is divided into $8 \times 8 \times 1=64$ elements. This mesh appears a good compromise between a sufficiently good precision and the time spent to solve the numerical problem.

Reference dimensions and values of the elastic moduli are shown in Table 3 (numerical *input* data for the calculation code). The value of applied forces F is 10 N.

In Figs. 12 and 13, the predominant stress field curves predicted theoretically (light lines, see Table 2) are compared with those obtained numerically (dark lines). As can be seen, theoretical and numerical analysis agree satisfactorily.

Focusing attention on the stress peak, the theory developed in the investigation predicts a peak value of:

$$\sigma_{y\max}^{theory}=\left|\sigma_y\left(x=\pm c,\ z=\pm\frac{b}{2}\right)\right|=1807 \cdot 10^3 \text{ Pa} \tag{23}$$

whereas the value resulting from numerical analysis is:

$$\sigma_{y\max}^{num}=1878 \cdot 10^3 \text{ Pa} \tag{24}$$

Table 3 Reference dimensions and elastic moduli

a (mm)	b (mm)	c (mm)	h (mm)	E_a^* (GPa)	E (GPa)	ν
3	20	10	0.3	1	45	0.31

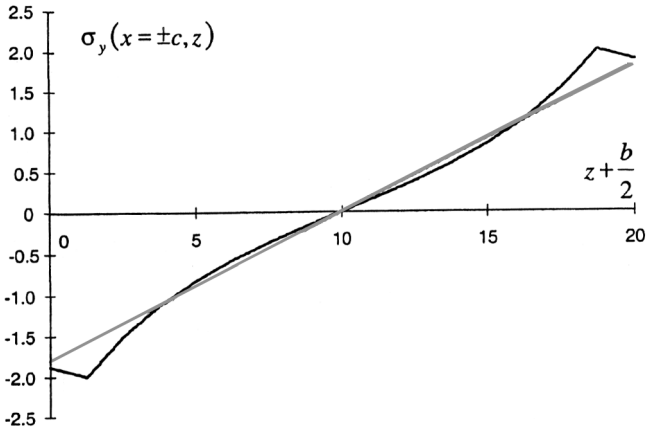

Fig. 12 Comparison between numerical (black line) and theoretical (grey line) transverse stress field curves, (end planes $x=\pm c$). Predominant stress (MPa)-Position in bond (mm)

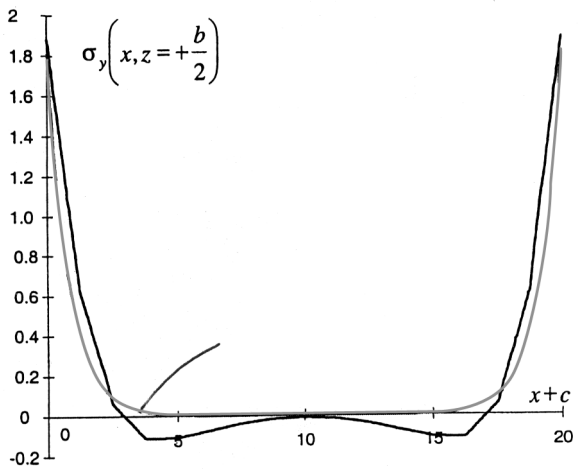

Fig. 13 Comparison between numerical (black line) and theoretical (grey line) longitudinal stress field curves, (critical planes $z = \pm b/2$). Predominant stress (MPa)-Position in bond (mm)

The relative error on the stress peak is thus:

$$e=\frac{\sigma_{y\max}^{num}-\sigma_{y\,\max}^{theory}}{\sigma_{y\max}^{num}}=3.78\% \tag{25}$$

The difference between numerical and theoretical approaches can be justified remembering the simplified hypothesis took into account in the theory developed. In particular the inversion of the sign of the predominant stress, varying the x co-ordinate, obtained from the numerical approach is not obtained using the theoretical approach. However we must remember as this component of the stress is an order of magnitude less than the stress peak.

This comparison shows as the theory developed can be used to estimate the predominant stress

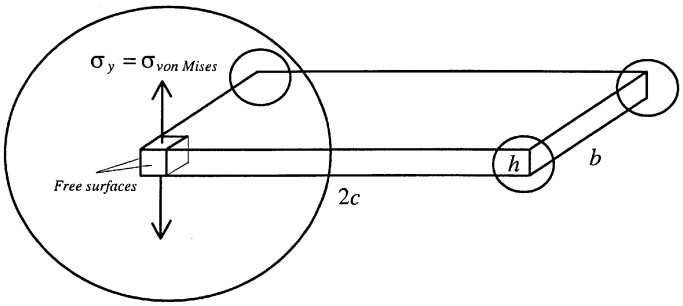

Fig. 14 Predominant and von Mises stresses at the corners of the adhesive ($x=\pm c$, $z=\pm b/2$)

field and its stress peaks at the four corners of the adhesive in a non-tubular bonded joint subjected to torsion. Theoretical and numerical approaches agree satisfactorily.

To determine the non-predominant stress fields we would have to remove the kinematic hypotesis, but, in any case, the von Mises equivalent stress at the most highly stressed points, the four corners of the adhesive (Pugno 1998), can be estimated by calculating the peak stress of the predominant field σ_y; indeed at the corners of the adhesive the predominant and von Mises stresses are coincident (Fig. 14).

However, it is important to note that adhesive bonded joints, non-tubular ones in particular, are by nature susceptible to brittle collapse. If no appropriate technological measures are introduced to ensure that joint collapse cannot involve mechanical fracture phenomena, brittle collapse will precede tensile collapse. Starting from the elastic analysis (that shows the points of high stress-concentration in the adhesive from where the cracks propagate) it is possible to predict the brittle collapse of the joint, in agreement with the experimental results (Pugno 1998).

6. Conclusions

The analytical relations which describe the static torsional problem for adhesive bonded *single-lap* joints were determined on the basis of reasonable simplifying assumptions. Considering equilibrium and compatibility, and assuming linear elastic constitutive laws, the analytical relations governing torsional moment transmission in the joint, the predominant interface stress field and the elastic strain in the joint were determined in closed form.

The procedure used was validated by comparing the theoretical stress field in the adhesive with the stress field obtained following three dimensional finite element analysis.

Acknowledgements

The authors would like to thank Prof. A. Manuello and Dr. D. Rittatore for their contribution in the numerical analysis, Prof. Carpinteri, Dr. C. Surace and the Italian National Research Council (CNR) and the Fiat Research Centre (CRF) for funding the work described in this paper.

References

Adams, R.D. and Peppiatt, N.A. (1977), "Stress analysis of adhesive bonded tubular lap joints", *J. Adhesion*, **9**, 1-18.

Alwar, R.S. and Nagaraja, Y.R. (1976), "Viscoelastic analysis of an adhesive tubular joint", *J. Adhesion*, **8**, 79-92.

Bryant, R.W. and Dukes, W.A. (1965), "The measurement of the shear strenght of adhesive joints in torsion", *Brit. J. Appl. Phys.*, **16**, 101-108.

Chen, D. and Cheng, S. (1992a), "Torsional stress in tubular lap joints", *Int. J. Solids and Structures*, **29**, 845-853.

Chen, D. and Cheng, S. (1992b), "Torsional stresses in tubular lap joints with tapered adherends", *J. Engineering Mechanics, ASCE,* **118**, 1962-1973.

Choi, J.H. and Lee, D.G. (1994), "The torque transmission capabilities of the adhesively-bonded tubular single lap joint and the double lap joint", *J. Adhesion,* **44**, 197-212.

Chon, C.T. (1982), "Analysis of tubular lap joint in torsion", *J. Composite Materials,* **16**, 268-284.

Gent, A.N. and Yeoh, O.H. (1982), "Failure loads for model adhesive joints subjected to tension, compression or torsion", *J. Materials Science,* **17**, 1713-1722.

Graves, S.R. and Adams, D.F. (1981), "Analysis of a bonded joint in a composite tube subjected to torsion", *J. Composite Materials,* **15**, 211-224.

Hipol, P.J. (1984), "Analysis and optimization of a tubular lap joint subjected to torsion", *J. Composite Materials,* **18**, 298-311.

Jeong, K.S., Lee, D.G., Kwak, Y.K. (1995), "Application of adhesive joining technology for manufacturing of the composite flexspline for a harmonic drive", *J. Adhesion,* **48**, 195.

Kim, K.S., Kim, W.T., Lee, D.G., Jun, E.J. (1992), "Optimal tubular adhesive-bonded lap joint of the carbon-fiber epoxy composite shaft", *Composite Structures,* **21**, 163-176.

Kim, W.T. and Lee, D.G. (1995), "Torque transmission capabilities of adhesively bonded tubular lap joints for composite drive shafts", *Composite Structures,* **30**, 229-240.

Lee, D.G., Kim, K.S., Im, Y.T. (1991), "An experimental-study of fatigue-strength for adhesively bonded tubular single lap joints", *J. Adhesion,* **35**, 39-53.

Lee, S.J. and Lee, D.G. (1992), "Development of a failure model for the adhesively bonded tubular single lap joint", *J. Adhesion,* **40**, 1-14.

Lee, S.J. and Lee, D.G. (1995), "An iterative solution for the torque transmission capability of adhesively-bonded tubular single lap joints with nonlinear shear properties", *J. Adhesion,* **53**, 217-227.

Lee, S.W., Lee, D.G. and Jeong, K.S. (1997), "Static and dynamic torque characteristics of composite cocured single lap joint", *J. Composite Materials,* **31**, 2188-2201.

Lubkin, J.L. and Reissner, E. (1956), "Stress distribution and design data for adhesive lap joints between circular tubes", *Trans. ASME,* **78**, 1213-1221.

Matsui, K. (1991), "Size effects on nominal ultimate shear stresses of adhesive-bonded circular or rectangular joints under torsion", *Int. J. Adhesion and Adhesives,* **11**, 59-64.

Matsui, K., Ueda, Y., Aihara, Y. and Miyazaki, H. (1986), "Size-effect on ultimate shear stress of adhesive-bonded tubular lap or tubular butt or circular scarf butt joint under twisting load", *J. Adhesion Soc. Japan,* **22**, 479-483.

Matsui, K., Ueda, Y., Morikawa, Y. and Yoshino, T. (1987), "Size-effect on ultimate torsional stress of adhesive-bonded joint with a rectangular cross section", *J. Adhesion Soc. Japan,* **23**, 96-102.

Medri, G. (1977), "Il calcolo delle tensioni nell'adesivo in giunti tra tubi sollecitati da momento torcente", *Ingegneria Meccanica,* 7/**8**, 247-251.

Medri, G. (1988), "Viscoelastic analysis of adhesive bonded lap joints between tubes under torsion", *J. of Vibration Acoustics Stress and Reliability in Design-Transactions, ASME,* **110**, 384-388.

Moloney, A.C., Kausch, H.H. and Stieger, H.R. (1984), "The use of the double torsion test geometry to study the fracture of adhesive joints", *J. Materials Science letters,* **3**, 776-778.

Nayebhashemi, H., Rossettos, J.N. and Melo, A.P. (1997), "Multiaxial fatigue life evaluation of tubular adhesively bonded joints", *Int. J. Adhesion and Adhesives,* **17**, 55-63.

Prakash, V., Chen, C.M., Engelhard, A. and Powell, G. (1995), "Torsional fatigue test for adhesive-bonded butt joints", *J. Testing and Evaluation,* **23**, 228-230.
Pugno, N. (1998), "Non tubular bonded joints under torsion", Ph.D. Thesis, Dept. of Structural Engineering, Politecnico di Torino, Torino, Italy.
Pugno, N. (1999), "Optimizing a non-tubular adhesive bonded joint for uniform torsional strength", *Int. J. of Materials and Product Technology*, **14**, 476-487.
Pugno, N. and Surace, G. (1998a), "Ottimizzazione di un giunto incollato tubular-lap progettato ad uniforme resistenza a torsione", *Proceedings of XXVII AIAS*, 1043-1052, Perugia, Italy.
Pugno, N. and Surace, G. (1998b), "Theoretical tensional analysis of a single lap bonded joint subjected to torsion", *Proceedings of VII NMCM,* 189-195, Hihg Tatras, Slovak Republic.
Pugno, N. and Surace, G. (1998c), "Analisi teorica tensionale di un giunto incollato double-lap soggetto a torsione", *Proceedings of XXVII AIAS,* 1053-1062, Perugia, Italy.
Rao, M.D. and Zhou, H. (1994), "Vibration and damping of a bonded tubular lap joint", *J. Sound and Vibration,* **178**, 577-590.
Reedy, E.D. and Guess, T.R. (1993), "Composite-to-metal tubular lap joints strength and fatigue resistance", *Int. J. Fracture,* **63**, 351-367.
Vonesebeck, G., Kising, M. and Neuhof, U., (1996), "Investigation on ceramic-metal joints for shaft-hub connections in gas-turbines", *J. of Engineering for Gas Turbines and Power-Transactions of the ASME,* **118**, 626-631.
Zhou, H.M. and Rao, M.D. (1993), "Viscoelastic analysis of bonded tubular joints under torsion", *Int. J. Solids and Structures,* **30**, 2199-2211.